2-2-2018

Aerobic Method for the Synthesis of Nearly Size-Monodisperse Bismuth Nanoparticles from a Redox Non-Innocent Precursor

Hayden Winter
Portland State University

Elena Christopher-Allison
Oregon State University/Oregon Health and Science University

Anna L. Brown
Portland State University

Andrea M. Goforth
Portland State University, amgofort@pdx.edu

Citation Details
Hayden Winter et al 2018 Nanotechnology in press.

Nanotechnology

Aerobic method for the synthesis of nearly size-monodisperse bismuth nanoparticles from a redox non-innocent precursor

To cite this article before publication: Hayden Winter *et al* 2018 *Nanotechnology* in press https://doi.org/10.1088/1361-6528/aaacb9

Aerobic method for the synthesis of nearly size-monodisperse bismuth nanoparticles from a redox non-innocent precursor

H Winter,[1] E Christopher-Allison,[1] A L Brown,[1,2,*] and A M Goforth[1*]

[1]Department of Chemistry, Portland State University, 1719 SW 10th Ave., Portland, OR 97201, USA

[2]Present address: College of Pharmacy, Oregon State University/Oregon Health and Science University, 2730 SW Moody Ave., Portland, OR 97201, USA

*Corresponding Authors

Abstract: Herein, we report an aerobic synthesis method to produce bismuth nanoparticles (Bi NPs) with average diameters in the range 40-80 nm using commercially available bismuth triiodide (BiI_3) as starting material; the method uses only readily available chemicals and conventional laboratory equipment. Furthermore, size data from replicates of the synthesis under standard reaction conditions indicate that this method is highly reproducible in achieving Bi NP populations with low standard deviations in the mean diameters. We also investigated the mechanism of the reaction, which we determined results from the reduction of a soluble alkylammonium iodobismuthate precursor species formed *in situ*. Under appropriate concentration conditions of iodobismuthate anion, we demonstrate that burst nucleation of Bi NPs results from reduction of Bi^{3+} by the coordinated, redox non-innocent iodide ligands when a threshold temperature is exceeded. Finally, we demonstrate phase transfer and silica coating of the Bi NPs, which results in stable aqueous colloids with retention of size, morphology, and colloidal stability. The resultant, high atomic number, hydrophilic Bi NPs prepared using this synthesis method have potential for application in emerging X-ray contrast and X-ray therapeutic applications.

Introduction: Bismuth nanoparticles (Bi NPs) have garnered attention through the development of technologies ranging from nanoelectronics,[1–8] to catalysis,[9,10] to medical contrast agents.[11–21] For example, in the field of nanoelectronics, Bi NPs have been shown to be ideal catalysts for the growth of quantum-confined semiconductor nanowires (*e.g.,* of CdSe, ZnS) due to their low melting point and wide precursor miscibility, properties which facilitate vapor- or solution-liquid-solid growth of size-uniform, anisotropic nanostructures.[1,3,7] Additionally, elemental Bi NPs have demonstrated promise for use as blood-pool contrast agents in computed tomography (CT) X-ray imaging, as well as the possibility of enabling molecular X-ray imaging and providing radiation dose enhancement in cancer treatment.[13–21] Furthermore, our group has also realized the value of size-uniform Bi NPs that are miscible at high weight percent within a polymer matrix in the fabrication of flexible X-ray opaque shielding

materials.[22] Our ensuing work has thus focused on improving the synthesis of Bi NPs to achieve better size uniformity using more practical methods, which will be essential for the further exploration of these nanomaterials in an applied context.

Relative to the well-established synthesis methodology and excellent size uniformity achievable for some elemental NPs (*e.g.,* Ag, Au, and Pt NPs), the majority of Bi NP synthetic methods to date have resulted in relatively poor size or morphology control. Many challenges have been encountered in the synthesis of size-monodisperse Bi NPs, including the absence of commercially available starting materials that are highly soluble in traditional solvents. Furthermore, the low, but still thermodynamically favorable, reduction potential of Bi^{3+} is responsible for the ready environmental oxidation of Bi^0 once formed. Consequently, oxidative dissolution represents a challenge for the synthesis and storage of Bi NPs in aqueous solution, if the Bi NP surfaces are not well-protected against oxidants.

Previously, the production of size-uniform Bi NPs has been accomplished in several cases; these methods typically proceed *via* thermolysis of Bi^{3+} precursors in high boiling organic solvents.[1,2,6,8,9,15,23] Soluble precursors are necessary to achieve size-uniformity, and can be formed *in situ* by dissolving a bismuth salt in a coordinating ligand, such as oleylamine, or *ex-situ* using a coordinating ligand and a strong organic base such as *n*-BuLi.[24] To form size-uniform Bi NPs, the Bi^{3+} within the precursor must be rapidly reduced, leading to the buildup of Bi^0 monomer in solution and a burst nucleation of Bi NPs above a certain critical monomer concentration. To ensure a single nucleation event, and therefore a single size of NPs, this burst must occur under specific conditions, such as an activation temperature or upon the addition of a reducing agent.[25] For example, Kovalenko and coworkers accomplished burst nucleation through the injection of *n*-butyllithium (*n*-BuLi) into a solution of Bi(III)-oleylamine complex (prepared by dissolving $BiCl_3$ in oleylamine) at 160°C, and were able to produce highly size-uniform Bi NPs with average diameters between 10 and 21 nm, having standard deviations of ~6% of the mean diameter.[23] This method was also extensible to the synthesis of a variety of other metallic NPs. As a second example, Buhro and coworkers accomplished a burst nucleation synthesis of Bi NPs through the *ex situ* production of semi-stable bismuth(III) trimethylsilylamide ($Bi[N(SiMe_3)_2]_3$, prepared from $BiCl_3$, $Na[N(SiMe_3)_2]$, and *n*-BuLi) and its subsequent thermolysis in a non-coordinating solvent.[2] This method achieved highly size monodisperse Bi NPs with average

diameters tunable over a wide range of 3 – 115 nm and standard deviations of 5-10% of the mean diameter. Though these methods result in excellent size control, both are highly air-sensitive and performed under stringent air-free conditions.

Herein, we present a one-pot aerobic synthesis of Bi NPs in the size range 40-80 nm using commercially available BiI_3 as a precursor. Although similar to the two syntheses outlined above, the reaction requires neither high temperature injection of highly reactive chemicals, nor air sensitive precursors. Instead, our method takes advantage of the solubility and thermal instability of an iodobismuthate species generated *in situ* when BiI_3 is dissolved in a primary amine solvent, such as hexadecylamine (HDA), which allows the reaction to be performed in conventional glassware under ambient conditions. We further investigated the reproducibility of our method in producing ~60 nm diameter Bi NPs, and we have additionally examined the method scope (*i.e.,* parameter variation tolerance) and reaction mechanism by variation of the reaction conditions. Finally, we demonstrate the silica coating and phase exchange of ~60 nm diameter Bi NPs to aqueous solution. These results provide a simple synthesis method to produce monodisperse Bi NPs for further investigation in the biological and technological applications outlined above. For comparison with the method we present, Table S1 provides a survey of reagents, size and size polydispersity, and product solvent dispersibility information for a representative selection of prior methods that produce Bi NPs. Notably, different size ranges are afforded under different synthesis conditions, and aerobic syntheses are uncommon, as are hydrophilic products. To the best of our knowledge, this work describes for the first time the use of a redox non-innocent iodobismuthate precursor in the synthesis of Bi NPs.

Materials and Methods

Materials: The following chemicals were purchased and used without purification: For Bi NP synthesis, parameter variations, and controls: bismuth triiodide (BiI_3, 99.999%, Strem), bismuth tribromide ($BiBr_3$, 98%+, Sigma-Aldrich), bismuth trichloride ($BiCl_3$, 98%+, Acros), potassium hydroxide (KOH, 99%, VWR), di-isopropylbenzene (DIPB, 98%, 2:1 mixture of m and p isomers, Acros), 1-hexadecylamine (HDA, 90%, Technical Grade, Alfa Aesar), poly(1-vinylpyrrolidone)-graft-(1-triacontene) (PVPT, Sigma-Aldrich), hexane (ACS grade, mixture of isomers, Fisher), and ethanol (ACS grade, Fisher). For phase exchange: chloroform (ACS grade, Fisher), and poly(1-

vinylpyrrolidone) (PVP, 29k MW, Sigma-Aldrich). For silica coating: tetraethoxysilane (TEOS, 98%, Sigma-Aldrich), and ammonium hydroxide (NH_4OH, 30% aq. solution, Fisher). In the water control reaction, phase exchange, and silica coating procedure, electrophoretically pure water (18 MΩcm resistivity) was used. All reactions, purifications, and analyses were performed in ambient laboratory air and light conditions, unless otherwise indicated.

Standard synthesis conditions: All procedural steps were carried out in a chemical fume hood; caution must be taken due to the release of iodine (I_2) gas.

In a standard synthesis, 300 mg BiI_3 was loaded into a 100 mL one-neck round bottom flask and dispersed in 16 mL of DIPB. This suspension, containing colorless solvent and black BiI_3 as a dispersed solid powder, was stirred at 650 rpm and heated to 180°C for 15 minutes. At 180°C, I_2 was observed to evolve as a purple gas. A solution color change (to pale orange) was also observed, in addition to the formation of a brown-orange solid suspended in the mixture. The temperature was subsequently lowered to 100°C, followed by addition of 3.75 g of HDA and 345 mg of PVPT. This suspension was then stirred open to the atmosphere for 30 minutes, resulting in an orange opaque suspension. The flask was then closed to atmosphere and stirred at 100°C for an additional 30 minutes, during which time, no additional changes to the atmosphere in the flask were made. The temperature was then raised to 180°C over a period of 2.5 minutes. During heating, the orange solution color gradually intensified, and within seconds of reaching 180°C, became a homogeneous black colloid. The reaction was allowed to proceed at 180°C for 12.5 minutes before it was quenched (total reaction duration including heating interval = 15 minutes). To quench the reaction, the flask was removed from heat and cooled in a room temperature water bath for one minute. To isolate the Bi NPs, a 50 mL mixture of 1:1 hexane: ethanol was added to the reaction flask, followed by collecting the contents in a conical tube, sonicating for one minute, and centrifuging at 3000 rcf for 15 minutes. The Bi NPs were twice re-dispersed and centrifuged out of solution using 80 mL of 1:1 hexane: ethanol. The Bi NPs could then be stored, either as a stable colloid in toluene, or as a fully re-dispersible (in toluene) dry powder.

Variation of reagent quantities vs. the standard reaction conditions: Modifications to the standard reaction conditions were done to examine the parameter variation tolerance of the reaction. The reagent quantities used in individual parameter variation experiments are shown in Table S2.

Bi precursor substitution controls: In control experiments to determine the role of the bismuth starting material in the formation of Bi NPs produced under the standard conditions, the BiI_3 starting material was replaced with the same molar amount of bismuth oxyiodide (BiOI), $BiCl_3$, or $BiBr_3$. The remainder of the procedure remained the same, including the heating of only the starting material in DIPB at 180°C for 15 minutes. BiOI was prepared by dissolving 0.5 g of BiI_3 in 25 mL of aqueous 0.1 M KOH and briefly vortexing.[26] BiOI was collected by vacuum filtration.

Reagent exclusion controls: An HDA+PVPT exclusion control was run as follows: 300 mg BiI_3 was combined with 16 mL DIPB in a 100 mL round bottom flask and heated to 180°C for two hours. A purple gas was evolved from the flask, and over the course of two hours, an orange insoluble solid was formed. The reaction was cooled, and the solids were collected by brief centrifugation.

A DIPB+PVPT exclusion control was run as follows: BiI_3 and HDA were added to a 100 mL round bottom flask. This mixture was first heated at 100°C for 1 hour, resulting in an orange opaque suspension. After 1 hour, the reaction was closed to atmosphere and the temperature was increased to 180°C over a period of 2.5 minutes and held at 180°C for 12.5 minutes, followed by cooling in a water bath. The black insoluble reaction product was afterwards dispersed in 40 mL hexane and collected by brief centrifugation.

Oxygen exclusion and water addition controls: BiI_3 and HDA were added into two separate 100 mL, 2-neck round bottom flasks, each fitted with a stopper and a line valve. Each reaction mixture was freeze-pump-thawed three times (thawing at 50°C on a heating mantle) to remove atmospheric and dissolved oxygen, and subsequently back filled with argon and heated to 100°C for 1 hour. The oxygen exclusion control reaction was then heated to 180°C over a period of 2.5 minutes, and held at 180°C for 12.5 minutes, turning from an orange suspension to a black suspension after 3 minutes at the reaction temperature. After 12.5 minutes, the reaction progress was quenched by

cooling the reaction vessel in a water bath. Solid products were collected by centrifugation and washed with 1:1 ethanol: hexane.

For the water addition control, the same steps were taken as in the oxygen exclusion control, except that 100 μL H_2O was added after 1 hour of heating at 100°C. The water addition control was next heated at 180°C for 1 hour, which did not result in the formation of Bi^0, but rather in the formation of an orange precipitate.

Surface modification to accomplish phase transfer to aqueous solution: To achieve phase transfer of the PVPT-coated Bi NPs to water, it was necessary to further coat the as-prepared nanoparticles with hydrophilic, unmodified PVP. To accomplish this, ~100 mg of Bi NPs (a typical yield when using the standard reaction conditions) were dispersed in 50 mL of chloroform by sonication, followed by the addition of one gram of PVP (29k MW) to the flask. The solution was subsequently stirred and refluxed for ~10 hours, and afterwards, the Bi NPs were collected by centrifugation. Excess PVP was removed by twice re-dispersing the Bi NPs in 25 mL of ethanol followed by centrifugation. The solid obtained by centrifugation was then dried in air at 125°C for 15 minutes.

Silica coating: Dry PVP-coated Bi NPs (~20 mg) were dispersed in a solution containing 90 mL ethanol and 10 mL deionized H_2O by sonicating the mixture for ~30 minutes. Subsequently, 2 mL of 30% aqueous NH_4OH and then 25 μL of TEOS were added while stirring. Stirring was continued for 30 minutes at room temperature, and then the flask was moved to a 4°C freezer and cooled for ~15 hours. Afterwards, silica-coated Bi NPs were collected by centrifugation. The silica-coated Bi NPs were isolated by twice re-dispersing them in 25 mL of ethanol followed by centrifugation, then dried at 80°C.

Crystallographic, microscopic, and spectroscopic characterizations of Bi NPs: Bi NP imaging was performed on a Technai F20 TEM operating at 4500 eV and equipped with an Oxford Instruments EDX detector. Samples were prepared by drop casting Bi NP dispersions in toluene (~4 mg/mL) onto type-B carbon-coated copper TEM grids (Ted Pella product #1844-F). Samples were allowed to air-dry for at least 10 minutes at room temperature followed by at least 5 minutes at 125°C. Images were processed using the FIJI software package. All mean diameter and standard deviation data was derived from at least 200 NP diameter measurements per synthesis. For any TEM image used, all NPs in the image were included to eliminate selective measuring.

X-ray diffraction (XRD) samples were prepared by drying Bi NPs or other solid precipitates in a drying oven at 125°C, then grinding them into a fine powder using a mortar and pestle. These powders were then placed in a zero-background (Si (100)) micro-holder slide. Characterization was performed using a Rigaku Ultima IV X-ray diffraction system in focused beam (Bragg-Brentano) geometry with graphite monochromatized Cu K_{alpha} radiation.

FT-IR spectra were obtained using a Thermo Scientific Nicolet iS10 spectrometer fitted with an attenuated total reflectance attachment having a diamond window. Solid samples were first dried of solvents by heating at 125°C, then placed directly on the diamond window and compressed.

Results and Discussion:

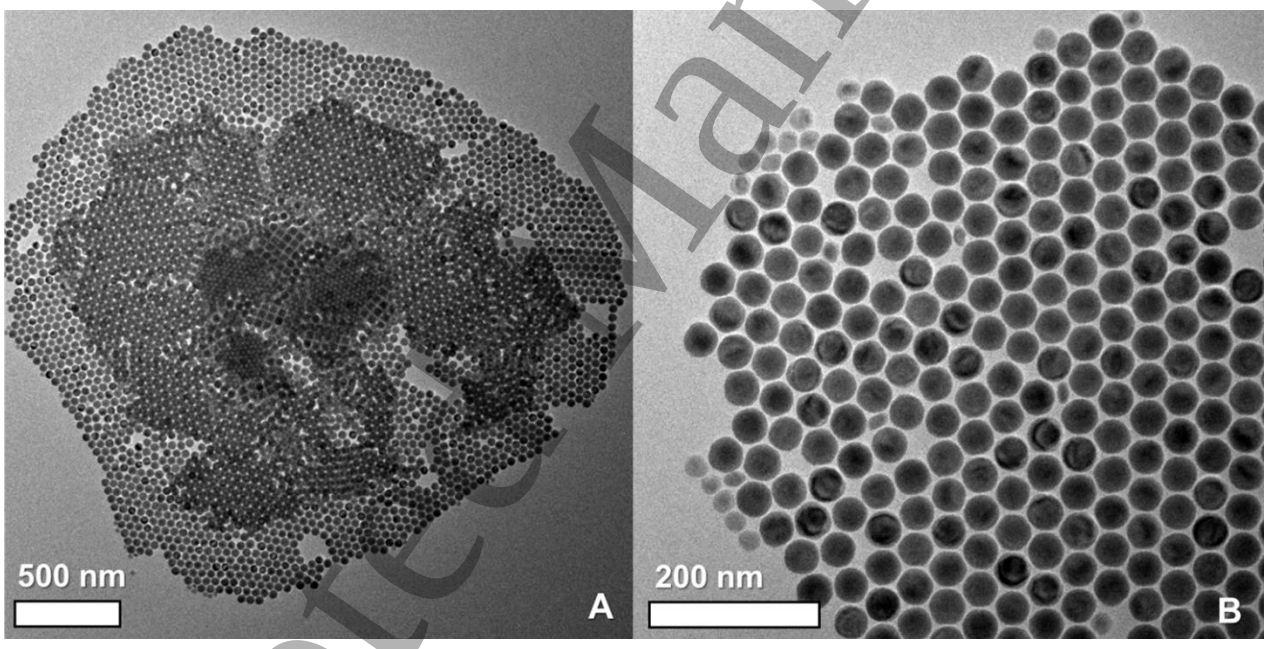

Figure 1. TEM images of Bi NPs from Sample 1 of the replicate experiments with scale bars of A) 500 nm and B) 200 nm.

Using a one-pot aerobic method, highly size and shape-monodisperse Bi NPs have been synthesized using commercially available bismuth triiodide (BiI_3) as starting material. As we support by mechanistic studies (*vide infra*), Bi NPs are formed through the thermolysis of a dissolved iodobismuthate precursor in a high-boiling solvent mixture of di-isopropylbenzene (DIPB) and hexadecylamine (HDA), in the presence of a polymeric surface-stabilizing agent, poly(1-vinylpyrrolidone)-*graft*-(1-triacontene) (PVPT). As a result of the triacontene chains of

the PVPT on the surface, the as-prepared Bi NPs are hydrophobic and readily dispersed as stable colloids in toluene, hexane, or other apolar solvents.

Table 1. Size and polydispersity data from five replicate syntheses of Bi NPs using the standard reaction conditions. For Samples 1-5, greater than 200 NPs per sample were measured from various areas of the TEM images.

Sample Number	Mean Diameter (nm)	Standard Deviation (nm)	% Std. Dev.
1	37.0	5.9	15.9
2	60.3	9.8	16.3
3	49.7	4.1	8.2
4	77.9	11.1	14.2
5	67.4	8.7	12.9
Pooled (1-5)	64.8	11.9	18.3

Using the standard reaction conditions (with respect to reagent quantities, see Table S2), the product Bi NPs were observed by TEM to have spherical morphologies, a mean diameter between 40 nm and 80 nm that varies between replicate syntheses, and low percent standard deviations in the mean diameters for each replicate synthesis. Table 1 contains size and standard deviation statistics for five replicates of the standard reaction conditions, which were performed over a time period spanning 5 months. Overall, the low standard deviations, which are between 8% and 17% of their respective population mean diameters, lead us to categorize the products of individual replicate syntheses as being nearly size-monodisperse. As seen in Table 1, the most size-uniform replicate yielded Bi NPs with a mean diameter of 49.7 nm ± 4.1 nm (Sample 3, 8% std. dev.), while for a slightly more size-polydisperse sample (Sample 1, 16% std. dev.), Figure 1A and 1B show representative TEM micrographs in which a predominant population of ~40 nm diameter Bi NPs is apparent. In these images, a sparse population of ~20 nm Bi NPs is also observed. However, despite the presence of the sparse, smaller population, the larger population is size-monodisperse enough to produce regions of close-packed Bi NPs, which exclude the smaller population to the edges of the superlattice. The measured average inter-particle spacing between these close-packed Bi NPs is 2.2 nm,

which provides an estimate of the PVPT polymer coating thickness of 1.1 nm (*i.e.,* 2.2 nm divided by 2 particles). The TEM image of Sample 1 shown in Figure 1 is representative of the replicate samples produced using the standard reaction conditions (see Figure S1 for TEM of Samples 2-5), although the mean size and standard deviation were observed to vary between replicate syntheses. To illustrate the usefulness of this synthesis method in producing Bi NPs for biological or other applications, a simulated pooled batch was created by combining the TEM diameter data for 200 NPs from each replicate and treating the 1000 NP population as a single batch. This hypothetical pooled sample would result in a 64.8 nm ± 11.9 nm (18.3% std. dev.) Bi NP population that can still be considered to have low size-polydispersity.

Versus the standard reaction conditions, we performed additional experiments where we varied the quantities of HDA, BiI_3, and PVPT, as well as the reaction temperature and time, to determine size and size polydispersity trends as a function of these parameters (Table S2). In all of these experiments, the volume of DIPB solvent was held constant.

While the results of these variations are shown and discussed in greater detail in the Supporting Information, analysis of TEM images showed that reducing the HDA quantity to 50% did not result in the formation of Bi NPs, even when the reaction time was extended to 30 minutes, while reducing the HDA quantity to 75% of the standard quantity produced a bimodal distribution of Bi NP sizes with much greater polydispersity (79 ± 23 nm, 29% std. dev., Figure S2A) *vs.* the standard conditions. Conversely, increased amounts of HDA or BiI_3 resulted in diameter distributions at the high end of the range observed under the standard reaction conditions (*i.e.,* for 200% of the standard HDA quantity, 51 ± 9 nm, 18% std. dev., Figure S2B; for 125% of the standard BiI_3 quantity, 77 ± 10 nm, 13% std. dev., Figure S2D), while reducing the BiI_3 quantity to 50% resulted in highly monodisperse, disk-shaped Bi NPs (31 ± 2 nm, 6 % std. dev., Figure S2C). Overall, these results suggest that the reaction feasibility and size homogeneity of the Bi NP products have a greater dependence on the quantity of HDA than on the quantity of BiI_3, which prompted us to take a closer look at the reaction mechanism to examine the role of each reagent in the formation of Bi NPs.

In an experiment to determine if the reaction is feasible at lower temperatures, a synthesis under the standard conditions was performed at 170°C (Table S2). For this synthesis, a longer induction period (*i.e.,* 20 *vs.* 2.5 minutes) before appearance of a black colloid of Bi NPs indicated that the reaction is feasible at 170°C, while TEM imaging revealed a substantially widened size distribution (82±44 nm, 53% std. dev.) *vs.* synthesis at 180°C, which is likely attributable to a prolonged nucleation event. Temperature variants higher than 180°C were not performed since the size distributions at 180°C were relatively narrow, but the boiling point of the DIPB solvent is ~210°C, which may be considered a practical upper limit of synthesis temperature.

Finally, in experiments varying the reaction time while using standard reagent quantities, TEM images taken after reaction durations of 3 minutes, 10 minutes, 6 hours, and 20 hours (Figure S3) showed that Bi NP growth is complete after approximately 10 minutes, with little change in the population size statistics occurring between 10 minutes and 6 hours (see Table S2). However, for very long heating times, some further size changes that can be attributed to mass transfer between the nanoparticles is noticeable. These results indicate that PVPT is, as expected, an effective surface stabilizer for the Bi NPs, preventing rapid oxidative dissolution of the Bi NPs after they are formed.

Investigation of the Mechanism of Bi NP Formation: Using BiI_3, HDA, PVPT, and DIPB as reagents under the standard reaction conditions, the reaction was observed to occur in three distinct stages (Scheme 1). We further interrogated these stages to gain mechanistic understanding of the reaction.

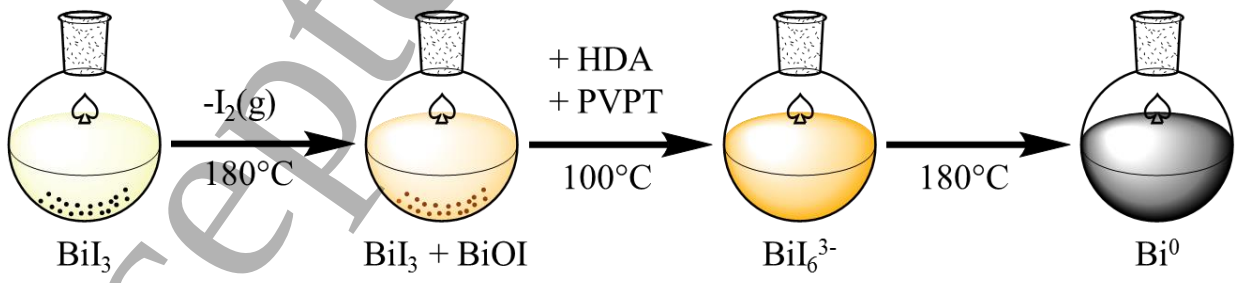

Scheme 1. Proposed identities of the predominant bismuth species in the three different stages of the reaction.

In the first stage of the reaction, BiI_3 was suspended in DIPB and heated to 180°C for 15 minutes while open to ambient atmosphere. At first, no significant dissolution of the solid or change in solution color was observed (Figure 2A); however, upon heating to 180°C, the formation of I_2 was observed as an evolving purple gas (Figure 2B). Additionally, during this initial heating interval, a pale yellow-orange solution containing an orange insoluble solid was formed (Figure 2C), and the solid was identified by powder X-ray diffraction (XRD) as bismuth oxyiodide (BiOI). In a separate HDA+PVPT exclusion control, we determined that heating BiI_3 in only DIPB at 180°C did not produce elemental Bi within 2 hours, although a greater mass of BiOI was produced with extended heating (Figure 3A, PDF Card 9009164).

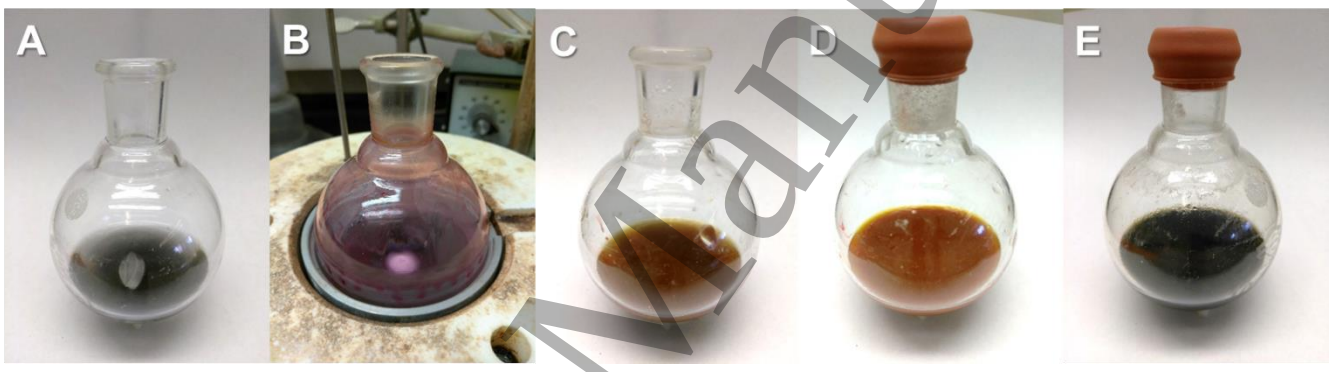

Figure 2. Photographs of the Bi NP synthesis at different procedural points. (A) BiI_3 in DIPB prior to heating. (B) I_2 gas being released from a mixture of BiI_3 in DIPB at 180°C. (C) Reaction solution after 15 minutes at 180°C. (D) Reaction solution after addition of HDA and PVPT and 1 hour of heating at 100°C. (E) Bi NP colloid formed after heating mixture in "D" at 180°C for 15 minutes including the heat ramping interval.

The second stage was initiated by lowering the reaction temperature to 100°C, at which point PVPT and HDA were added. After these additions, the reaction was held at 100°C for 1 hour, during which time a bright orange solution containing an orange precipitate was formed (Figure 2D). The reaction mixture was subsequently increased in temperature to 180°C to initiate the third stage, which resulted in the rapid loss of both orange solution color and solid to yield a homogeneous black solution of colloidal Bi NPs (Figure 2E). XRD analysis of the final product showed that the NPs produced under the standard reaction conditions are composed of highly crystalline rhombohedral Bi^0 (Figure 3B, PDF Card 2310889). A separate DIPB+PVPT exclusion control containing only BiI_3 and HDA was run in air at 180°C, initially resulting in the formation of a bright orange solution and orange precipitate, which quickly darkened to a black suspension within 3 minutes and produced bulk, elemental Bi rather

than Bi NPs. From the results of the HDA+PVPT and DIPB+PVPT exclusion control reactions, it can be concluded that DIPB and PVPT function only to modulate the growth of the Bi NPs, and that only BiI_3 and HDA are necessary to produce Bi^0. The roles of DIPB and PVPT in the reaction are therefore to control the soluble precursor concentration and to limit the growth of the Bi NPs, respectively.

In further equimolar substitution controls to examine the role of the halide in the starting material, we determined that BiOI and $BiBr_3$ can be used as alternate starting materials to produce Bi NPs under the standard reaction conditions. Interestingly, Bi NPs produced using $BiBr_3$ as a precursor had a mixture of spherical and cuboid morphologies as shown in Figure S4. However, a control experiment using $BiCl_3$ as precursor failed to produce Bi^0. In light of the result that iodide- and bromide-containing salts produce Bi^0, while chloride-containing salts do not, it can be concluded that the identity of the halide ion is pivotal in the reduction of Bi^{3+}.

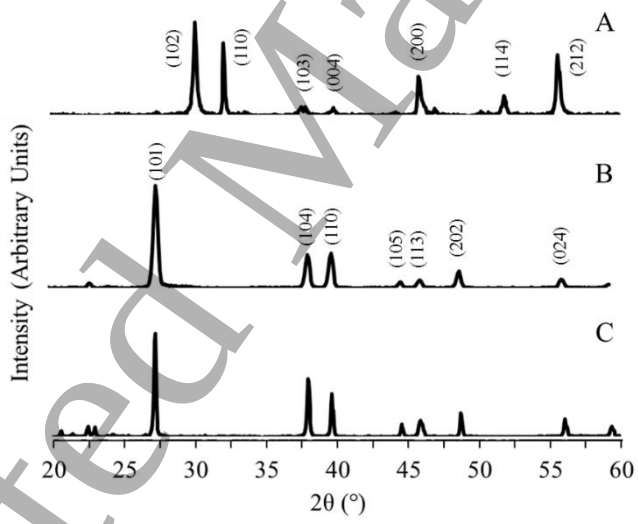

Figure 3. XRD patterns of solids collected from Bi NP synthesis and control experiments. (A) BiOI produced by heating BiI_3 in DIPB only. (B) Bi NPs from Sample 2, produced under the standard reaction conditions. (C) Bulk Bi^0 recovered from the oxygen exclusion control in the absence of DIPB and PVPT.

Examination of the literature provides support for the identity of the soluble, orange precursor as an anionic iodobismuthate species. A large number of halobismuthate salts containing a variety of anions are known, *e.g.,* discrete $Bi_2X_9^{3-}$, $Bi_3X_{11}^{2-}$, $Bi_4X_{16}^{4-}$, $Bi_6X_{22}^{4-}$, and polymeric BiX_4^- and BiX_5^{2-} (X = Cl, Br, or I),[27–30] and such anions are generally polynuclear, being composed of corner or edge-sharing BiX_6^{3-} octahedra. Frequently, ammonium cations

provide charge balance for the polynuclear halobismuthate anions in these salts, although sometimes cations are generated *in situ via* the formation of Bi^{3+}-solvent complexes.[31]

Though the precise composition of the proposed iodobismuthate solution precursor was not identified, the characteristic orange color of the solution observed during the second stage of the reaction is likely due to a ligand-to-metal charge transfer (LMCT) transition between iodide ligands and coordinated Bi^{3+} cation(s).[29,32–36] The observation that our standard reaction conditions result in elemental bismuth when using BiI_3, BiOI, or $BiBr_3$ as starting materials, but not when using $BiCl_3$, indicate that the LMCT is responsible for initiating Bi^0 formation at a reaction temperature of 180ºC. This observation is consistent with the lower bond and LMCT energies reported for iodo- *vs.* bromo- *vs.* chlorobismuthate compounds. Typically reported bond energies are highest for Bi-Cl at ~300 kJ/mol and lowest for Bi-I at ~190 kJ/mol,[37,38] and values for the energies of the LMCT transitions are known to be red-shifted for iodo- *vs.* bromo- *vs.* chlorobismuthates.[32,35,39] For example, for a series of compounds containing $BiCl_6^{3-}$, $BiBr_6^{3-}$, and BiI_6^{3-} anions, the lowest energy spectral feature assigned as LMCT is present at 231 nm (X = Cl) *vs*. 274 nm (X = Br) *vs*. 412 nm (X = I).[40] Thus, under the standard conditions of our aerobic synthesis, it can be inferred that iodide anions are complexed with the Bi^{3+} ions until reduction and behave as non-innocent ligands in the reduction of Bi^{3+} to form Bi NPs.

Under the standard reaction conditions, protonated HDA is the likely counter-cation for the iodobismuthate anion that is formed *in situ*. Both as-received HDA and DIPB contain trace water, and were not purified prior to use; thus, trace water is expected to protonate HDA to some extent. Supportive of the formation of an alkylammonium iodobismuthate precursor *en route* to Bi NPs, FT-IR spectroscopy of the reaction products prior to isolation by centrifugation (Figure S5) indicates the formation of hexadecylammonium, as evidenced by a broad peak at 3031 cm^{-1} that is characteristic of N-H bonding in primary ammonium species. The role of hexadecylammonium cations in charge balancing iodobismuthate anions formed *in situ* is also consistent with the qualitative observation that the intensity of the orange color, assigned as an I-Bi LMCT, increases upon HDA addition, due to increasing iodobismuthate concentration in solution. Here, it should be noted that the orange solution color indicative of

iodobismuthate was also formed in DIPB, although to a lesser extent and apparently at an insufficient concentration to initiate particle nucleation at 180ºC.

Of importance for both Bi NP size-homogeneity and reaction feasibility is the concentration of the soluble iodobismuthate species, which is expected to be modulated by the concentration of protonated HDA. The protonated HDA concentration is expected to be affected by the concentration of water, which can not only protonate HDA but also reduce solution concentrations of Bi^{3+} and I^- ions in the formation of BiOI (*i.e.,* reaction of BiI_3 with H_2O is used to quantitatively prepare BiOI) or other precipitates (*vide infra*). Thus, a water addition control reaction was performed.

In the water addition control reaction, BiI_3 and HDA were first heated at 100°C for one hour to produce a bright orange solution, followed by injection of 0.1 mL of water into the flask. Upon water addition, the orange solution color was observed to decrease in intensity and the formation of a brown-orange precipitate was observed. Afterwards, the temperature of the solution was increased to 180°C and held for one hour; however, no color change was observed. The precipitate recovered at the end of one hour at the reaction temperature was analyzed by XRD (Figure S6), and neither Bi^0 or BiOI could be identified. The brown-orange polycrystalline solid was not further characterized, but is likely a hexadecylammonium iodobismuthate salt with low crystallographic symmetry. These results indicate that very high cation concentrations are correlated to high iodobismuthate anion concentrations, sufficient to result in salt precipitation at 100°C. Conversely, when there is not enough water or protonated cation present, as is likely in the case of heating BiI_3 in DIPB only, insufficient iodobismuthate precursor is formed, and nucleation also does not occur at 180°C. A water exclusion control reaction was not done, since this synthesis method produces low-polydispersity Bi NP samples in ambient, humidified air. However, based on the result in DIPB only, we would expect that use of completely anhydrous conditions would also effectively lower the solution concentration of the iodobismuthate precursor and prevent nucleation of Bi^0 NPs at 180°C. Overall, the high degree of water sensitivity could explain the batch-to-batch variability observed when using hygroscopic solvents in ambient humidity conditions, suggesting that to improve batch-to-batch size variability, the water content should be measured and kept consistent between replicate syntheses.

A further oxygen exclusion control reaction was also done using only HDA as solvent. Prior to heating, the flask containing only HDA and BiI_3 was freeze-pump-thawed to remove O_2, and subsequently kept under an argon atmosphere. Just as in air, a bright orange solution was produced at 100°C, followed by a rapid color change from orange to black upon increasing the temperature to 180°C. The black solid isolated from this reaction was identified as Bi^0 by XRD (Figure 3C). We can conclude from this experiment that atmospheric oxygen neither promotes, nor inhibits, the reduction of the iodobismuthate precursor.

Phase transfer and silica coating: The as-prepared PVPT-coated Bi NPs are readily dispersible in nonpolar solvents (*e.g.,* toluene), and therefore of use to researchers interested in catalysis or quantum wire growth. However, in order to obtain water-soluble Bi NPs for biological applications, and to prevent rapid oxidative dissolution when dispersed as an aqueous colloid, additional surface treatments were necessary. Consequently, the as prepared PVPT-coated Bi NPs were first pre-coated with hydrophilic PVP, then subsequently coated with a thin silica shell. Silica surfaces are useful for further functionalization of NPs using widely available and simplistic silane conjugation techniques.[41–44]

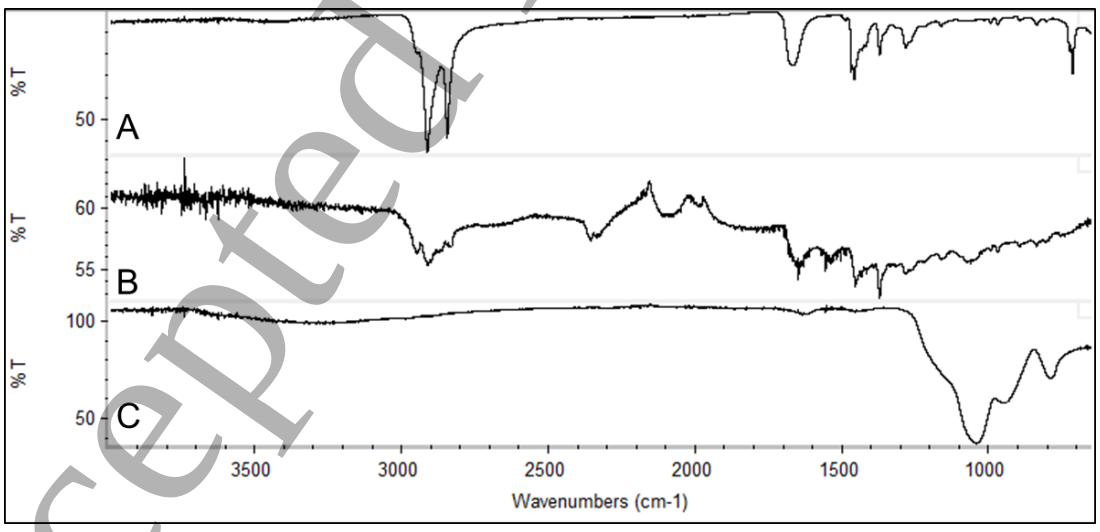

Figure 4. FT-IR spectra of as-prepared Bi NPs (A), Bi NPs after additional PVP pre-treatment (B), and Bi NPs after silica coating (C).

To accomplish this, the hydrophobic PVPT-coated Bi NPs were first pre-coated in PVP by refluxing the as-prepared Bi NPs in chloroform containing 29k MW PVP. This treatment yielded hydrophilic Bi NPs which could be dispersed as a stable colloid in the polar solvents which make up the Stöber environment (*i.e.,* aqueous NH_3 and ethanol), in which a silica shell can be deposited. Comparison of the FT-IR spectra of as-prepared Bi NPs (Figure 4A) *vs.* Bi NPs after pre-treatment with PVP (Figure 4B) reveal a difference in the intensity ratio of sp^3 C-H stretching (2916cm^{-1}) to sp^2 C-O stretching (1653 cm^{-1}), which is expected for the addition of unmodified PVP to the triacontene-bearing PVPT on the as-prepared Bi NP surfaces. TEM imaging established that the Bi NPs retained their original core size distribution and morphology during this phase transfer step, and also established that there is not observable degradation of the surfaces in an aqueous environment (Figure S7).

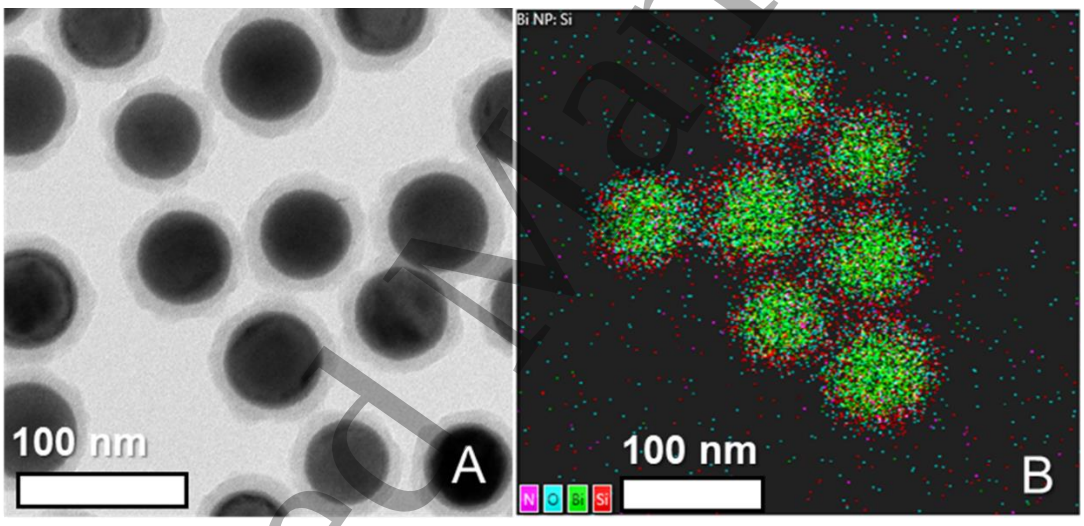

Figure 5. A) TEM image showing Bi NPs with silica coatings. B) EDX compositional map of Bi NPs with silica coatings.

Following pre-treatment with unmodified PVP, Bi NPs coated could then be put in a Stöber environment, in which NH_4OH hydrolyses TEOS, producing SiO_2 that is deposited onto the Bi NP surfaces. Through optimization of water to ethanol ratios, TEOS amounts, and reaction time, we identified parameters that result in a thin ~10 nm silica layer on the majority of the recovered Bi NPs (Figure 5A). However, co-encapsulation of multiple Bi NPs into a single SiO_2 shell was sparsely observed. The FT-IR spectrum of the resulting silica-coated Bi NPs (Figure 4C) shows a strong absorbance at 1045 cm^{-1} from Si-O stretching. EDX compositional mapping was also used to confirm the

identity of the coating as silica, with silicon and oxygen characteristic X-rays being emitted from the areas outside of the bismuth cores (Figure 5B). The silica-coated Bi NPs were readily dispersible in water (pH ~7) as a stable black colloid, which showed no signs of significant degradation or dissolution over the course of two months.

Conclusion: Nearly monodisperse Bi NPs with sizes between 40 and 80 nm were synthesized through an aerobic reaction of bismuth triiodide in hexadecylamine and di-isopropylbenzene, using a hydrophobic polymer to prevent aggregation and oxidative dissolution. In this reaction, a soluble iodobismuthate anion forms *in situ* and serves as both oxidant and reductant in the formation of Bi NPs, resulting from burst nucleation and growth due to thermolysis of the iodobismuthate. The method is simple and reproducible, with an average standard deviation in the mean diameter of ~14% over five replicate syntheses. While in-batch variability in size was observed to be low, batch-to-batch variability in the mean population diameter was relatively high (± 20 nm over 5 syntheses). We attribute this to the variable concentration of alkylammonium cation that provides charge balance for the iodobismuthate anion, which is sensitive to the water content of the reaction.

The as-prepared Bi NPs produced by this method were coated in PVP-graft-triacontene, making them highly dispersible in nonpolar solvents, and therefore of use to researchers interested in templating quantum wires. Surface treatment with PVP and silica coating procedures have also been performed to result in water-dispersible Bi NPs with retention of size, morphology and colloidal stability. Our future work will focus on further improving the batch-to-batch consistency of the Bi NP synthesis as well as evaluation of their biocompatibility and X-ray attenuation properties.

ASSOCIATED CONTENT

Supporting Information: Comparison of other literature preparations of Bi NPs *vs.* this work; reagent quantities and size distributions for replicate, parameter modification, and control experiments; TEM micrographs of all standard condition replicates; TEM micrographs and histograms from parameter modification studies; a detailed analysis of the parameter modification results; TEM micrograph of Bi NPs produced using $BiBr_3$ as precursor; FT-IR spectra of neat hexadecylamine compared to hexadecylammonium from un-isolated Bi NP products; XRD pattern of the unidentified solid from the water addition control; and a TEM micrograph of PVP-coated Bi NPs are provided.

AUTHOR INFORMATION

Corresponding Author

* agoforth@pdx.edu

* broanna@ohsu.edu

Author Contributions

The manuscript was written through contributions of all authors. All authors have given approval to the final version of the manuscript.

Funding Sources

This work was supported by the Burroughs Wellcome Fund (Award Number 1007294.01, A.M.G.), and the Oregon Nanoscience and Microtechnologies Institute (A.M.G) and *via* start-up funds from Portland State University (A.M.G.). We also acknowledge the National Science Foundation for XRD instrumentation (NSF-MRI, Award Number DMR- 0923572).

ACKNOWLEDGMENTS

We acknowledge the Center for Electron Microscopy and Nanofabrication at Portland State University for their assistance in TEM characterization.

REFERENCES

(1) Wang, F.; Buhro, W. E. An Easy Shortcut Synthesis of Size-Controlled Bismuth Nanoparticles and Their Use in the SLS Growth of High-Quality Colloidal Cadmium Selenide Quantum Wires. *Small* **2010**, *6* (4), 573–581.

(2) Wang, F.; Tang, R.; Yu, H.; Gibbons, P. C.; Buhro, W. E. Size- and Shape-Controlled Synthesis of Bismuth

Nanoparticles. *Chem. Mater.* **2008**, *20* (11), 3656–3662.

(3) Fanfair, D. D.; Korgel, B. A. Bismuth Nanocrystal-Seeded III-V Semiconductor Nanowire Synthesis. *Cryst. Growth Des.* **2005**, *5* (5), 1971–1976.

(4) Heremans, J.; Thrush, C. Thermoelectric Power of Bismuth Nanowires. *Phys. Rev. B* **1999**, *59* (19), 12579–12583.

(5) Hostler, S. R.; Qu, Y. Q.; Demko, M. T.; Abramson, A. R.; Qiu, X.; Burda, C. Thermoelectric Properties of Pressed Bismuth Nanoparticles. *Superlattices Microstruct.* **2008**, *43* (3), 195–207.

(6) Son, J. S.; Park, K.; Han, M. K.; Kang, C.; Park, S. G.; Kim, J. H.; Kim, W.; Kim, S. J.; Hyeon, T. Large-Scale Synthesis and Characterization of the Size-Dependent Thermoelectric Properties of Uniformly Sized Bismuth Nanocrystals. *Angew. Chemie - Int. Ed.* **2011**, *50* (6), 1363–1366.

(7) Wang, F.; Wayman, V. L.; Loomis, R. A.; Buhro, W. E. Solution-Liquid-Solid Growth of Semiconductor Quantum-Wire Films. *ACS Nano* **2011**, *5* (6), 5188–5194.

(8) Yarema, M.; Kovalenko, M. V.; Hesser, G.; Talapin, D. V.; Heiss, W. Highly Monodisperse Bismuth Nanoparticles and Their Three-Dimensional Superlattices. *J. Am. Chem. Soc.* **2010**, *132* (43), 15158–15159.

(9) Wang, Z.; Jiang, C.; Huang, R.; Peng, H.; Tang, X. Investigation of Optical and Photocatalytic Properties of Bismuth Nanospheres Prepared by a Facile Thermolysis Method. *J. Phys. Chem. C* **2014**, *118* (2), 1155–1160.

(10) Pothula, K.; Tang, L.; Zha, Z.; Wang, Z. Bismuth Nanoparticles: An Efficient Catalyst for Reductive Coupling of Nitroarenes to Azo-Compounds. *RSC Adv.* **2015**, *5* (101), 83144–83148.

(11) Swy, E. R.; Schwartz-Duval, A. S.; Shuboni, D. D.; Latourette, M. T.; Mallet, C. L.; Parys, M.; Cormode, D. P.; Shapiro, E. M. Dual-Modality, Fluorescent, PLGA Encapsulated Bismuth Nanoparticles for Molecular and Cellular Fluorescence Imaging and Computed Tomography. *Nanoscale* **2014**, *6* (21), 13104–

13112.

(12) Hahn, M. A.; Singh, A. K.; Sharma, P.; Brown, S. C.; Moudgil, B. M. Nanoparticles as Contrast Agents for *in vivo* Bioimaging: Current Status and Future Perspectives. *Anal. Bioanal. Chem.* **2011**, *399* (1), 3–27.

(13) Lusic, H.; Grinstaff, M. W. X-Ray-Computed Tomography Contrast Agents. *Chem. Rev.* **2013**, *113* (3), 1641–1666.

(14) Cormode, D. P.; Naha, P. C.; Fayad, Z. A. Nanoparticle Contrast Agents for Computed Tomography: A Focus on Micelles. *Contrast Media Mol. Imaging* **2014**, *9* (1), 37–52.

(15) Wei, B.; Zhang, X.; Zhang, C.; Jiang, Y.; Fu, Y. Y.; Yu, C.; Sun, S. K.; Yan, X. P. Facile Synthesis of Uniform-Sized Bismuth Nanoparticles for CT Visualization of Gastrointestinal Tract *in vivo*. *ACS Appl. Mater. Interfaces* **2016**, *8* (20), 12720–12726.

(16) Brown, A. L.; Naha, P. C.; Benavides-Montes, V.; Litt, H. I.; Goforth, A. M.; Cormode, D. P. Synthesis, X-Ray Opacity, and Biological Compatibility of Ultra-High Payload Elemental Bismuth Nanoparticle X-Ray Contrast Agents. *Chem. Mater.* **2014**, *26* (7), 2266–2274.

(17) Jakhmola, A.; Anton, N.; Vandamme, T. F. Inorganic Nanoparticles Based Contrast Agents for X-Ray Computed Tomography. *Adv. Healthc. Mater.* **2012**, *1* (4), 413–431.

(18) Chen, G.; Roy, I.; Yang, C.; Prasad, P. N. Nanochemistry and Nanomedicine for Nanoparticle-Based Diagnostics and Therapy. *Chem. Rev.* **2016**, *116* (5), 2826–2885.

(19) Lei, P.; An, R.; Zhang, P.; Yao, S.; Song, S.; Dong, L.; Xu, X.; Du, K.; Feng, J.; Zhang, H. Ultrafast Synthesis of Ultrasmall Poly(Vinylpyrrolidone)-Protected Bismuth Nanodots as a Multifunctional Theranostic Agent for *in vivo* Dual-Modal CT/Photothermal-Imaging-Guided Photothermal Therapy. *Adv. Funct. Mater.* **2017**, *1702018*, 1702018.

(20) Yu, X.; Li, A.; Zhao, C.; Yang, K.; Chen, X.; Li, W. Ultrasmall Semimetal Nanoparticles of Bismuth for

Dual-Modal Computed Tomography/Photoacoustic Imaging and Synergistic Thermoradiotherapy. *ACS Nano* **2017**, *11* (4), 3990–4001.

(21) Li, Z.; Liu, J.; Hu, Y.; Li, Z.; Fan, X.; Sun, Y.; Besenbacher, F.; Chen, C.; Yu, M. Biocompatible PEGylated Bismuth Nanocrystals: "All-in-One" Theranostic Agent with Triple-Modal Imaging and Efficient *in vivo* Photothermal Ablation of Tumors. *Biomaterials* **2017**, *141*, 284–295.

(22) Goforth, A.; Brown, A. Bismuth Particle X-Ray Contrast Agents. U.S. Patent Application No. 14/124236. 2014.

(23) He, M.; Protesescu, L.; Caputo, R.; Krumeich, F.; Kovalenko, M. V. A General Synthesis Strategy for Monodisperse Metallic and Metalloid Nanoparticles (In, Ga, Bi, Sb, Zn, Cu, Sn, and Their Alloys) via *in situ* Formed Metal Long-Chain Amides. *Chem. Mater.* **2015**, *27* (2), 635–647.

(24) Mourdikoudis, S.; Liz-Marzán, L. M. Oleylamine in Nanoparticle Synthesis. *Chem. Mater.* **2013**, *25* (9), 1465–1476.

(25) Wu, Z.; Yang, S.; Wu, W. Shape Control of Inorganic Nanoparticles from Solution. *Nanoscale* **2016**, *8* (3), 1237–1259.

(26) Brauer, G. Handbook of Preparative Inorganic Chemistry. *Acad. Press (New York, N.Y.)* **1965**, 625.

(27) Greenwood, N. N.; Earnshaw, A. *Chemistry of the Elements*, 2nd ed.; Elsevier: Oxford, 1995; Vol. 2.

(28) Lindsjö, M.; Fischer, A.; Kloo, L. Anionic Diversity in Iodobismuthate Chemistry. *Zeitschrift fur Anorg. und Allg. Chemie* **2005**, *631* (8), 1497–1501.

(29) Goforth, A. M.; Tershansy, M. A.; Smith, M. D.; Peterson, L. R.; Kelley, J. G.; DeBenedetti, W. J. I.; zur Loye, H. C. Structural Diversity and Thermochromic Properties of Iodobismuthate Materials Containing D-Metal Coordination Cations: Observation of a High Symmetry $[Bi_3I_{11}]^{2-}$ Anion and of Isolated I-Anions. *J. Am. Chem. Soc.* **2011**, *133* (3), 603–612.

(30) Wu, L. M.; Wu, X. T.; Chen, L. Structural Overview and Structure-Property Relationships of Iodoplumbate and Iodobismuthate. *Coord. Chem. Rev.* **2009**, *253* (23–24), 2787–2804.

(31) Goforth, A. M.; Peterson, L. R.; Smith, M. D.; zur Loye, H. C. Syntheses and Crystal Structures of Several Novel Alkylammonium Iodobismuthate Materials Containing the 1,3-*bis*-(4-Piperidinium)propane Cation. *J. Solid State Chem.* **2005**, *178* (11), 3529–3540.

(32) Mason, W. R. Electronic Absorption and MCD Spectra for BiX_6^{3-}, X = Cl -, Br -, and I -, in Acetonitrile Solution: Metal-Centered vs Ligand-to-Metal Charge-Transfer Assignments. *Inorg. Chem.* **1999**, *38* (11), 2742–2745.

(33) Brütsch, L.; Feldmann, C. One-Pot Photoinitiated Synthesis and Phase-Transfer Separation of Bismuth Nanoparticles. *Zeitschrift für Anorg. und Allg. Chemie* **2017**.

(34) Maurer, A. B.; Hu, K.; Meyer, G. J. Light Excitation of a Bismuth Iodide Complex Initiates I-I Bond Formation Reactions of Relevance to Solar Energy Conversion. *J. Am. Chem. Soc.* **2017**, *139* (24), 8066–8069.

(35) Oldenburg, K.; Vogler, A.; Mikó, I.; Horváth, O. Photoredox Decomposition of tin(II), lead(II), antimony(III) and bismuth(III) Iodide Complexes in Solution. *Inorganica Chim. Acta* **1996**, *248* (1), 107–110.

(36) Tershansy, M. A.; Goforth, A. M.; Gardinier, J. R.; Smith, M. D.; Peterson Jr., L.; zur Loye, H. . Solvothermal Syntheses, High- and Low-Temperature Crystal Structures, and Thermochromic Behavior of [1,2-Diethyl-3,4,5-Trimethyl-Pyrazolium]$_4$ [Bi_4 I_{16}] and [1,10-phenanthrolinium][BiI_4]-(H_2O). *Solid State Sci.* **2007**, *9*, 410–420.

(37) Haynes, W. M. *CRC Handbook of Chemistry and Physics*; 2014.

(38) Luo, Y.-R. *Comprehensive Handbook of Chemical Bond Energies*; CRC Press, 2007.

(39) Ferjani, H.; Boughzala, H.; Driss, A. Synthesis, Crystal Structure and Characterization of a New Organic-Inorganic Hybrid Material: $(H_3AEP)_2$-$(BiCl_6)^-$3Cl-2H_2O. *J. Crystallogr.* **2013**, *2013*, 26–32.

(40) Horváth, O.; Mikó, I. Spectra, Equilibrium and Photoredox Chemistry of Iodobismuthate(III) Complexes in Acetonitrile. *Inorganica Chim. Acta* **2000**, *304* (2), 210–218.

(41) Kango, S.; Kalia, S.; Celli, A.; Njuguna, J.; Habibi, Y.; Kumar, R. Surface Modification of Inorganic Nanoparticles for Development of Organic-Inorganic Nanocomposites - A Review. *Prog. Polym. Sci.* **2013**, *38* (8), 1232–1261.

(42) Fonseca, L. C.; de Paula, A. J.; Martinez, D. S. T.; Alves, O. L. How Does the Chain Length of PEG Functionalized at the Outer Surface of Mesoporous Silica Nanoparticles Alter the Uptake of Molecules? *New J. Chem.* **2016**, *40* (9), 8060–8067.

(43) Plueddemann, E. P. Chemistry of Silane Coupling Agents. In *Silane Coupling Agents*; Springer US: Boston, MA, 1991; pp 31–54.

(44) Chakravarty, S.; Unold, J.; Shuboni-Mulligan, D. D.; Blanco-Fernandez, B.; Shapiro, E. M. Surface Engineering of Bismuth Nanocrystals to Counter Dissolution. *Nanoscale* **2016**, *8* (27), 13217–13222.

(45) Chen, X.; Chen, S.; Huang, W.; Zheng, J.; Li, Z. Facile Preparation of Bi Nanoparticles by Novel Cathodic Dispersion of Bulk Bismuth Electrodes. Electrochim. Acta 2009, 54, 7370–7373.